Absence of midgap states due to excess electrons donated by adsorbed hydrogen on the anatase TiO_2(101) surface

Naoki Nagatsuka,[1] Koichi Kato,[1] Markus Wilde,[1] and Katsuyuki Fukutani[1,2]
[1]*Institute of Industrial Science, The University of Tokyo, 4-6-1 Komaba Meguro-ku, Tokyo 153-8505, Japan*
[2]*Advanced Science Research Center, Japan Atomic Energy Agency (JAEA), Tokai, Ibaraki 319-1195, Japan*

(Received 2 September 2021; revised 9 November 2021; accepted 13 January 2022; published 28 January 2022)

Hydrogen is involved in various important chemical processes on metal-oxide surfaces. Due to its electron-donating character, hydrogen tends to form polaronic states, where the electron is spatially separated from the proton, which exerts significant impact on the electronic properties of metal-oxide surfaces. By individually probing the proton with nuclear reaction analysis and the electron with ultraviolet photoelectron spectroscopy and in combination with density functional theory calculations, we clarify the electronic state of hydrogen on the anatase TiO_2(101) surface. Hydrogen is found to adsorb with a saturation coverage of 0.48 ± 0.12 monolayers, donating an excess electron to the substrate without forming a midgap state, which is in contrast to the behavior of oxygen vacancies.

DOI: 10.1103/PhysRevB.105.045424

Titanium dioxide (TiO_2) finds many applications including photocatalytic water splitting and hydrogen sensors. Understanding the interaction of hydrogen (H) with TiO_2 surfaces is thus of crucial importance to elucidate the microscopic mechanisms behind these functionalities [1,2]. In ionic crystals, the introduction of defects such as oxygen vacancies (V_O) and interstitial hydrogen produces excess electrons, which often form localized states accompanied by lattice distortion through electron-phonon interaction (EPI) [3], so-called polarons. Depending on the strength of the EPI, polaronic states are classified into small and large (Fröhlich) polarons: in the former, the electron is localized at a specific site, while in the latter the electron extends over several unit cells, propagating through the lattice with an increased effective mass. These quasiparticles are formed in a variety of materials such as transition metal oxides [4–7], organic semiconductors [8] and two-dimensional materials [9], exerting significant effects on the charge transport properties [8,10] and surface reactivity [11,12]. A typical metal oxide is TiO_2, and it has been reported that excess electrons form different polaronic states on the surfaces of the rutile and anatase polymorphs of TiO_2. The polaronic character may well depend on if a polaron is formed at the surface or in bulk. Focusing on the TiO_2 surfaces, it has been reported that excess electrons form different polaronic states on the rutile and anatase surfaces.

On the rutile TiO_2 (110) surface, ultraviolet photoemission spectroscopy (UPS) studies have revealed that excess electrons originating from V_O form midgap states at 0.8 eV below the Fermi level (E_F) [13–17]. These states mainly consist of Ti 3*d* orbitals as confirmed by resonant UPS [15], and are turned out to be localized at the Ti sites as small polarons as observed by scanning tunneling microscopy (STM) [7,18,19]. Therefore, the midgap state is regarded as a sign of small polaron formation. When the rutile TiO_2 (110) surface is exposed to atomic H, hydrogen adsorbs on the two-coordinated oxygen atoms (O_{2c}) that protrude from the surface [20–24], and the excess electron donated by the adsorbed H also forms a mid-gap state similar to V_O [25,26]. Hydrogen is also suggested to adsorb on the five-coordinated titanium atoms (Ti_{5c}) below 115 K [27]. The effects of V_O and adsorbed H on the electronic structure of the rutile TiO_2 (110) surface have also been analyzed theoretically. In order to examine the localized nature of excess electrons, the band gap of TiO_2 needs to be described correctly, which can be achieved by density functional theory (DFT) calculations using the $+U$ correction or hybrid functionals. DFT calculations with either +U correction or hybrid functional revealed the mid-gap state and localized nature of excess electrons due to V_O and adsorbed H are well reproduced on the (110) surface as well as in the bulk of rutile TiO_2 [28–39].

On anatase TiO_2, on the other hand, angle-resolved UPS has revealed that there exists a free-electron-like state near E_F on oxygen-deficient TiO_2 (101) and (001) surfaces, which are assigned to large polarons [40,41]. In addition to this free-electron-like state, a mid-gap state is also observed on anatase surfaces with V_O [41–43]. An STM study using scanning tunneling spectroscopy (STS) has found a mid-gap state localized near the V_O site. Although the large polaronic state due to V_O observed in photoelectron spectroscopy (PES) is not seen in STS, a shallow donor state bound to Nb dopants is observed in STM/STS on the Nb-doped anatase TiO_2(101) surface [7]. Considering the previous results of PES and STM/STS, it seems that both the delocalized state and mid-gap state coexist on the anatase TiO_2 surface with V_O in contrast to the rutile surface. A possible reason for the coexistence is that the first electron is localized at V_O forming a mid-gap state and the second electron is delocalized due to the Coulomb repulsion at V_O [44]. It is noted that coexistence of the free-electron-like state and mid-gap state was also observed at the oxygen-deficient and H-adsorbed $SrTiO_3$(001) surface [44–46]. It

should also be noted that observation of the free-electron-like state near E_F seems to depend on the experimental technique; it is invisible to STM [7] and UPS at a photon energy of 21.2 eV as shown later. Furthermore, the previous studies suggest that the electronic state of excess electrons is sensitive to the nature of the impurity, i.e., either V_O or Nb [7].

As to the H adsorption on the anatase TiO_2 surface, *ab initio* calculations have shown that H is adsorbed at the twofold O site and migrates to the subsurface region at high coverages [47,48]. While interstitial H in the anatase bulk is shown to form a mid-gap state [11,49–55], both possibilities of being localized at a single Ti atom and delocalization over several Ti atoms have been suggested by DFT calculations [11,30,31,33,34,49]. Experimentally, the dissociation of water at oxygen vacancies produces H atoms adsorbed at the two-coordinated oxygen atoms as confirmed by infrared reflection absorption spectroscopy [56]. Despite the importance of hydrogen on the anatase TiO_2 surface, however, the polaronic state of hydrogen-derived excess electron on the anatase TiO_2 surface is yet to be elucidated.

In the present study, we quantitatively measure the H coverage with nuclear reaction analysis (NRA) [57,58] and observe the electronic states with UPS on the clean and atomic H-exposed anatase TiO_2 (101) surface without oxygen vacancies. The NRA results show that H adsorbs on the surface with a saturation coverage of $(2.5 \pm 0.6) \times 10^{14}$ cm^{-2} (0.48 ± 0.12 ML; 1 ML $= 5.16 \times 10^{14}$ cm^{-2}). The adsorbed hydrogen donates an excess electron to the substrate as evidenced by band bending observed in UPS. In marked contrast to the rutile surface, no mid-gap states were observed due to H adsorption, which is also different from the behavior of oxygen vacancies on anatase surfaces. The absence of the mid-gap states suggests that the H-donated excess electron forms a large polaronic state.

The experiments were conducted in ultrahigh vacuum (UHV) chambers with base pressures below 1×10^{-8} Pa. The sample was a natural single-crystal anatase TiO_2(101), which was originally orange and partially blue in color. The surface was cleaned by 1 keV Ar^+ sputtering at 2 μA for 10 min followed by annealing at 600 °C under 1.0×10^{-4} Pa of oxygen (99.999 % purity) for 10 min. The sample shows electric conductivity, although no impurity is observed in x-ray photoelectron spectroscopy (XPS). H_2 gas (99.999%) was purified by a palladium membrane heated at 450 °C and introduced into the UHV chamber. Atomic hydrogen was produced by passing H_2 gas through a tungsten tube heated at 1650 °C. Hence, the sample surface was exposed to a mixture of hydrogen molecules and atomic hydrogen.

The surface electronic structure was investigated by UPS with the He I source (21.2 eV) in normal emission. The energy scale is referenced to the Fermi level of Au. The band bending and work function were evaluated from the shifts of the valence band maximum and the cutoff of the secondary-electron emission, respectively. The absolute density of H and its depth profile were evaluated by NRA via ^{1}H(^{15}N, $\alpha\gamma$) ^{12}C at room temperature at the 1E beamline of the 5 MV Van de Graaff Tandem accelerator in the Microanalysis Laboratory (MALT) of The University of Tokyo. The energy resonance of the ^{1}H(^{15}N, $\alpha\gamma$) ^{12}C reaction at 6.385 MeV has a width of 1.8 keV, which provides a few nm depth resolution. A $^{15}N^{2+}$ ion beam irradiated the sample surface at a current of 20-80 nA with a beam area of ~8 mm^2, and the γ ray from the nuclear reaction was detected with a $Bi_4Ge_3O_{12}$ scintillator [58]. The absolute density of H is evaluated by calibrating the γ-ray detection efficiency with a Kapton film of known H concentration. One concern of NRA is the damage due to the high-energy ^{15}N ion irradiation. It was confirmed that the signal intensity is almost the same before and after the depth profile measurement. According to the SRIM-2008 simulation software [59], furthermore, the N ion at an energy of 6.4 MeV has a penetration depth of 3.5 μm for the anatase TiO_2. This depth location is not expected to affect the surface properties. It was confirmed that the same UPS spectrum is observed and no impurities are observed in XPS after the NRA experiment. We can therefore safely consider that the N ion damage is neglected for the present experiment.

The hydrogen-adsorbed structure and the change of the work function were calculated based on DFT including on-site Coulomb interaction via a Hubbard term (DFT + U) with the PHASE code [60]. The exchange and correlation terms were expressed by the generalized gradient approximation (GGA) of Perdew-Burke-Ernzerhof [61]. The pseudopotential is employed with the projector augmented wave method. The cutoff energies are 25 Ry for the wave functions and 196 Ry for the augmented electron densities. The calculations were performed for seven layers with 4 k points for Brillouin-zone sampling. Inversion symmetry with respect to the slab center is used to enhance the computational efficiency. The structure model consists of a (2×2) surface unit cell and a slab of 7 layers with a vacuum spacing of the same thickness. The atomic positions are relaxed in order to reflect equilibrium positions. The value of U and the radius of the projection operator were determined such as to reproduce the experimental value of the band gap. We used $U = 4$ eV and a projection operator radius of 2.25 bohr.

Figure 1(a) demonstrates the changes of the UPS spectrum of the anatase TiO_2(101) surface due to exposure to atomic H. In Fig. 1(a), the predominant features between 3.5 and 9 eV are mainly derived from O 2p, where the three peaks at 4.5, 6.0, and 7.8 eV were assigned to the O 2p nonbonding, O 2p − Ti 3d π-bonding and O 2p-Ti 3d σ-bonding states, respectively [15]. After exposure to atomic hydrogen of 2000 Langmuir (1 Langmuir $= 1.33 \times 10^{-4}$ Pa · s), the spectrum shows a slight increase in the peak intensity around 9.6 eV. Since the H 1s-O 2p bonding orbital is expected to appear at 9–11 eV, H is adsorbed on the O atom. The spectrum also shows a downward shift of the O 2p band, implying that adsorbed H donates an excess electron to the surface and that the band is downward bent in the near-surface region. It is worth noting that no mid-gap state is present after exposure to atomic hydrogen in contrast to the rutile TiO_2(110) surface, where a mid-gap state was observed at 0.8 eV below the Fermi level [25,26]. The excess electron due to adsorbed H on anatase TiO_2(101) seems to form a large polaron state, although no significant intensity is observed at the Fermi level. Note that metallic states at the Fermi level are often invisible with UPS at 21.2 eV because of a small photoionization cross section [4], but may be observable at higher photon energies as demonstrated for the anatase TiO_2(101) and (001) surfaces with oxygen vacancies [41].

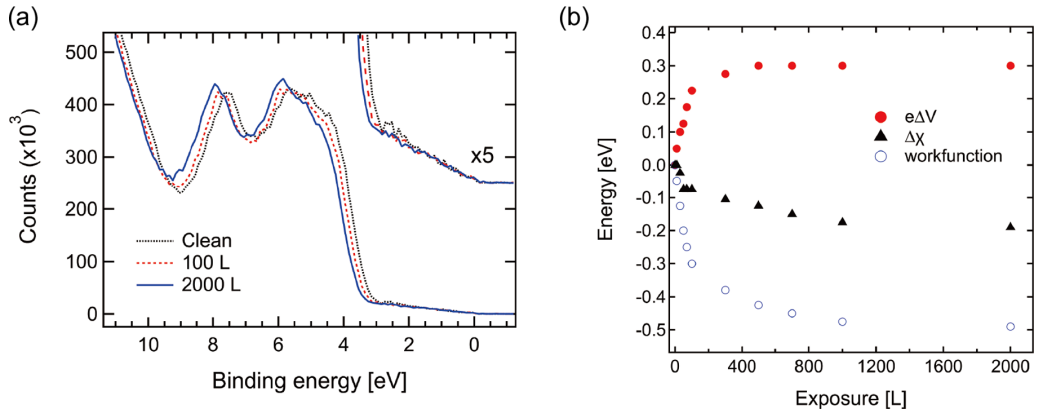

FIG. 1. (a) UPS spectra for clean and H exposed surfaces taken at room temperature with a photon energy of 21.2 eV. (b) Changes of the work function versus H exposure at 300 K. The band bending ($e\Delta V$) and the work function (ϕ) are estimated from UPS spectra. The electron affinity ($\Delta\chi$) is calculated from the relationship $\Delta\chi = \Delta\phi + e\Delta V$.

After electron irradiation with an energy of 500 eV at 102 K, on the other hand, a mid-gap state is observed at 1.1 eV below the Fermi level as shown in Fig. 2(a). Since electron irradiation induces oxygen vacancy formation, this mid-gap state originates from oxygen vacancies, which is consistent with previous studies [7,41]. Note that the O $2p$ band is also downward shifted after electron irradiation, indicating downward band bending. As shown in Fig. 2(a), the mid-gap state disappeared after heating the sample at 300 K for 10 min, which is consistent with a previous study showing that the oxygen vacancy migrates into the bulk around 200 K [62]. Figure 2(b) shows UPS spectra after electron irradiation at 300 K, where a mid-gap state was also observed in agreement with a previous study [42]. The electron irradiation dose required for the formation of the mid-gap state at 300 K was three times larger than that at 102 K. The results of Fig. 2 suggest that at 300 K the oxygen vacancy formation at the surface occurs after saturation of oxygen vacancies below the surface.

Figure 1(b) summarizes the changes of the band bending (eΔV), electron affinity ($\Delta\chi$), and work function ($\Delta\phi$) as a function of the H exposure at 300 K. The electron affinity is estimated from the relationship $\Delta\phi = -e\Delta V + \Delta\chi$. The work function and band bending steeply change up to 100 L followed by a gradual change with increasing H exposure. This indicates that electron donation from adsorbed H occurs continuously throughout the H exposure. Since the electron affinity reflects the surface dipole layer, the decrease in $\Delta\chi$ denotes formation of a dipole pointing to the vacuum, which is similar to the rutile TiO_2(110) surface [26]. The formation of a surface dipole throughout the H exposure suggests that the H atom mainly adsorbs on the bridging oxygen site forming an electric dipole pointing to the vacuum as shown in Fig. 4(a).

Figure 3(a) shows the NRA H depth profiles of the H-saturated anatase TiO_2(101) surface at 300 K and after heating in UHV to 500 and 700 K for 10 min. Only a symmetric peak centered at 0 nm is observed indicating the presence of H at the surface, while there is no absorbed H detectable in the subsurface region. The H density on the surface is estimated to be 0.48 ± 0.12 ML at saturation. After heating the sample, the intensity of the surface peak decreases at 500 K [Fig. 3(b)] and completely disappears upon heating at 700 K [Fig. 3(c)]. This temperature dependance is consistent with previous studies showing that adsorbed hydrogen desorbs around 500 K [56]. It should be noted, however, that the band bending was not recovered to the initial value after annealing at 700 K.

The adsorption structure and electronic state of hydrogen on the anatase TiO_2(101) surface were calculated by the DFT + U method with a U value of 4 eV. With this U value, the band gap was calculated to be 3.2 eV, which is

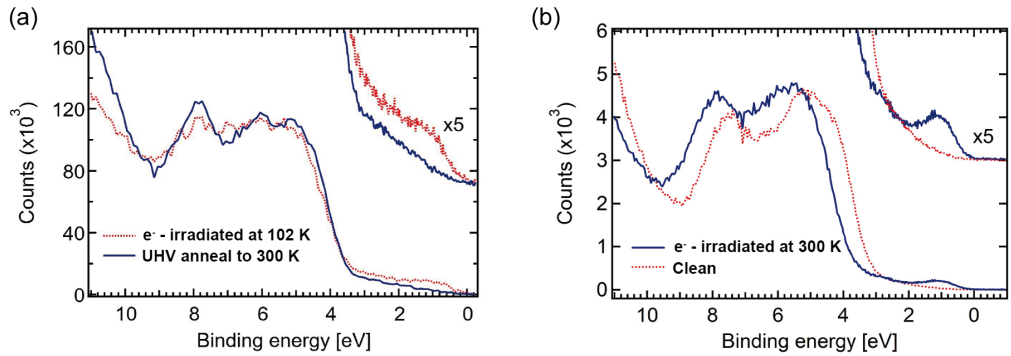

FIG. 2. (a) UPS spectra for surfaces after electron irradiation at 102 K and subsequent annealing at 300 K. (b) UPS spectra for clean and electron-irradiated surfaces taken at room temperature.

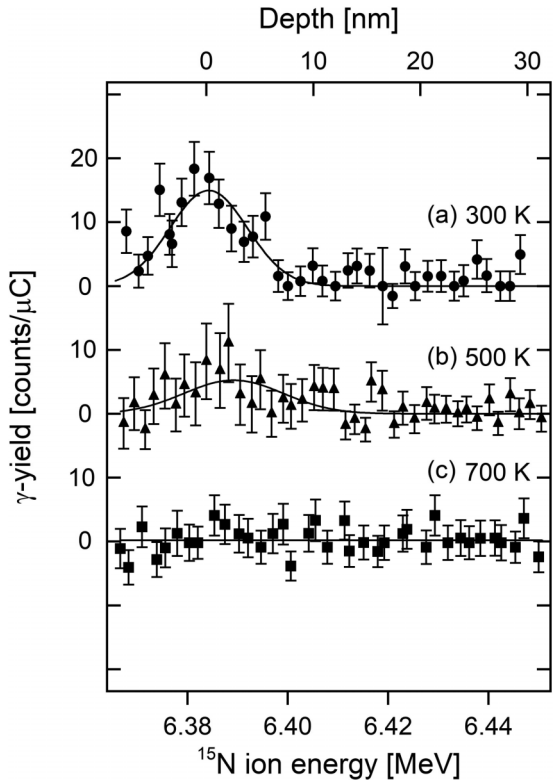

FIG. 3. NRA profiles for H-saturated surface at room temperature and after heating excursion to each temperature on anatase TiO_2(101) surfaces.

consistent with the experimental value. Figure 4(a) shows the side view of the H-adsorbed anatase TiO_2(101) surface and the calculated density of states. The conduction band has a tailing feature, and the H-related state is formed just below the conduction band minimum. The wave function corresponding to the excess electron is delocalized over several Ti atoms in the cell. This theoretical result is consistent with the present experimental results. The work function decrease calculated from the change in electron density [Fig. 4(b)] is 0.11 eV at 0.25 ML and 0.34 eV at 0.5 ML. This trend is in good agreement with the experimental results. Since the slab thickness used for the theoretical calculations is seven layers, the effect of band bending may not have been treated properly. This implies that the theoretical work-function value should rather be compared with the experimental electron affinity. Then the theoretical calculation seems to overestimate the work-function change compared with the experimental data. This difference may be caused by the difference in the electron density between the surface and the bulk, which means that U for the surface atoms should be smaller. In DFT, U corresponds to a part of the dynamically screened Coulomb interaction and is calculated as the difference between the on-site Coulomb interaction and the exchange interaction [63]. This means that U depends on the electron density, because the exchange interaction is proportional to the electron density to the power of one third.

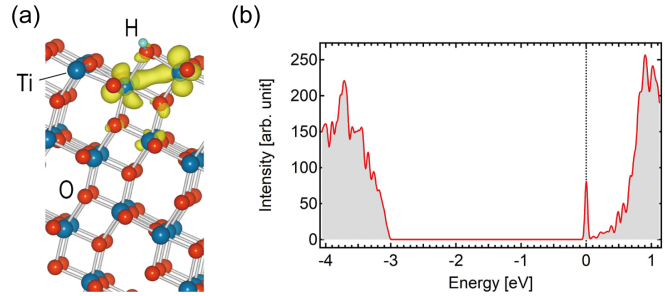

FIG. 4. (a) The side view of the calculated structure and charge densities of in-gap states of anatase TiO_2(101) surfaces where hydrogen adsorbed on an two-coordinated oxygen atom. Red, blue, and green balls represent O, Ti, and H atoms, respectively. Yellow isosurfaces represent electronic charges of excess electrons corresponding to the in-gap state. (b) Density of states calculated for the structure in Fig. 4(a). The dashed line indicates the Fermi level.

The mid-gap state is regarded as a fingerprint of a small polaron with a localized character of an excess electron. Whereas some theoretical studies showed presence of mid-gap states due to hydrogen adsorption on or interstitial hydrogen in anatase TiO_2 [47,50], other studies suggested both possibilities of localized and delocalized states for hydrogen-induced excess electrons [11,49]. The present study definitely shows that the excess electron due to hydrogen adsorption on the anatase TiO_2(101) surface reveals a delocalized character without forming a mid-gap state. This delocalized nature of the excess electron is related to a lower diffusion barrier of hydrogen in anatase TiO_2 as compared the rutile TiO_2 [64].

In conclusion, we have experimentally clarified the electronic state of hydrogen at the anatase TiO_2(101) surface with UPS and NRA. In combination with theoretical calculations, we have shown that the H-derived excess electrons form delocalized states on the anatase TiO_2(101) surface without forming a mid-gap state, which is in contrast to the excess electron behavior induced by oxygen vacancies.

The authors acknowledge the support from JSPS KAKENHI Grants No. JP18H05518, 21H04650 and 21K14588.

[1] A. Fujishimaand K. Honda, Electrochemical photolysis of water at a semiconductor electrode, Nature (London) **238**, 37 (1972).

[2] H. Tang, K. Prasad, R. Sanjinés, and F. Lévy, TiO_2 anatase thin films as gas sensors, Sens. Actuators B **26**, 71 (1995).

[3] C. Franchini, M. Reticcioli, M. Setvin, and U. Diebold, Polarons in materials, Nat. Rev. Mater. **6**, 560 (2021).

[4] A. F. Santander-Syro, O. Copie, T. Kondo, F. Fortuna, S. Pailhés, R. Weht, X. G. Qiu, F. Bertran, A. Nicolaou, A. Taleb-Ibrahimi, P. Le Févre, G. Herranz, M. Bibes, N. Reyren,

Y. Apertet, P. Lecoeur, A. Barthélémy, and M. J. Rozenberg, Two-dimensional electron gas with universal subbands at the surface of $SrTiO_3$, Nature (London) **469**, 189 (2011).

[5] E. Possenriede, H. Kröse, T. Varnhorst, R. Scharfschwerdt, and O. F. Schirmer, Shallow acceptor and electron conduction states in $BaTiO_3$, Ferroelectrics **151**, 199 (1994).

[6] W.-J. Yin, B. Wen, C. Zhou, A. Selloni, and L.-M. Liu, Excess electrons in reduced rutile and anatase TiO_2, Surf. Sci. Rep. **73**, 58 (2018).

[7] M. Setvin, C. Franchini, X. Hao, M. Schmid, A. Janotti, M. Kaltak, C. G. Van de Walle, G. Kresse, and U. Diebold, Direct View at Excess Electrons in TiO_2 Rutile and Anatase, Phys. Rev. Lett. **113**, 086402 (2014).

[8] V. Coropceanu, J. Cornil, D. A. da Silva Filho, Y. Olivier, R. Silbey, and J.-L. Brédas, Charge transport in organic semiconductors, Chem. Rev. **107**, 926 (2007).

[9] M. Kang, S. W. Jung, W. J. Shin, Y. Sohn, S. H. Ryu, T. K. Kim, M. Hoesch, and K. S. Kim, Holstein polaron in a valley-degenerate two-dimensional semiconductor, Nat. Mater. **17**, 676 (2018).

[10] Y. Furubayashi, T. Hitosugi, Y. Yamamoto, K. Inaba, G. Kinoda, Y. Hirose, T. Shimada, and T. Hasegawa, A transparent metal: Nb-doped anatase tio_2, Appl. Phys. Lett. **86**, 252101 (2005).

[11] C. Di Valentin, G. Pacchioni, and A. Selloni, Reduced and n-Type Doped TiO_2 : Nature of Ti^{3+} Species, J. Phys. Chem. C **113**, 20543 (2009).

[12] U. Aschauer, Y. He, H. Cheng, S.-C. Li, U. Diebold, and A. Selloni, Influence of subsurface defects on the surface reactivity of TiO_2: Water on anatase (101), J. Phys. Chem. C **114**, 1278 (2010).

[13] V. E. Henrich, G. Dresselhaus, and H. J. Zeiger, Observation of Two-Dimensional Phases Associated with Defect States on the Surface of TiO_2, Phys. Rev. Lett. **36**, 1335 (1976).

[14] U. Diebold, The Surface Science of Titanium Dioxide, Surf. Sci. Rep. **48**, 53 (2003).

[15] A. G. Thomas, W. R. Flavell, A. K. Mallick, A. R. Kumarasinghe, D. Tsoutsou, N. Khan, C. Chatwin, S. Rayner, G. C. Smith, R. L. Stockbauer, S. Warren, T. K. Johal, S. Patel, D. Holland, A. Taleb, and F. Wiame, Comparison of the electronic structure of anatase and rutile TiO_2 single-crystal surfaces using resonant photoemission and x-ray absorption spectroscopy, Phys. Rev. B **75**, 035105(2007).

[16] C. M. Yim, C. L. Pang, and G. Thornton, Oxygen Vacancy Origin of the Surface Band-Gap State of TiO_2(110), Phys. Rev. Lett. **104**, 036806 (2010).

[17] Y. Ohashi, N. Nagatsuka, S. Ogura, and K. Fukutani, Hydrogen distribution and electronic structure of TiO_2(110) hydrogenated with low-energy hydrogen ions, J. Phys. Chem. C **123**, 10319 (2019).

[18] T. Minato, Y. Sainoo, Y. Kim, H. S. Kato, K.-i. Aika, M. Kawai, J. Zhao, H. Petek, T. Huang, W. He, B. Wang, Z. Wang, Y. Zhao, J. Yang, and J. G. Hou, The electronic structure of oxygen atom vacancy and hydroxyl impurity defects on titanium dioxide (110) surface, J. Chem. Phys. **130**, 124502 (2009).

[19] C. M. Yim, M. B. Watkins, M. J. Wolf, C. L. Pang, K. Hermansson, and G. Thornton, Engineering Polarons at a Metal Oxide Surface, Phys. Rev. Lett. **117**, 116402 (2016).

[20] S. Suzuki, K.-I. Fukui, H. Onishi, and Y. Iwasawa, Hydrogen Adatoms on TiO_2(110)(1x1) Characterized by Scanning Tunneling Microscopy and Electron Stimulated Desorption, Phys. Rev. Lett. **84**, 2156 (2000).

[21] V. E. Henrichand R. L. Kurtz, Surface electronic structure of TiO_2: Atomic geometry, ligand coordination, and the effect of adsorbed hydrogen, Phys. Rev. B **23**, 6280 (1981).

[22] J. Pan, B. L. Maschhoff, U. Diebold, and T. E. Madey, Interaction of water, oxygen, and hydrogen with TiO_2(110) surfaces having different defect densities, J. Vac. Sci. Thechnol. A **10**, 2470 (1992).

[23] M. Kunat, U. Burghaus, and C. Wöll, The adsorption of hydrogen on the rutile TiO_2(110) surface, Phys. Chem. Chem. Phys. **6**, 4203 (2004).

[24] X.-L. Yin, M. Calatayud, H. Qiu, Y. Wang, A. Birkner, C. Minot, and C. Wöll, Diffusion versus Desorption: Complex Behavior of H Atoms on an Oxide Surface, ChemPhysChem **9**, 253 (2008).

[25] X. Mao, X. Lang, Z. Wang, Q. Hao, B. Wen, Z. Ren, D. Dai, C. Zhou, L.-M. Liu, and X. Yang, Band-gap states of TiO_2(110): Major contribution from surface defects, J. Phys. Chem. Lett. **4**, 3839 (2013).

[26] K. Fukada, M. Matsumoto, K. Takeyasu, S. Ogura, and K. Fukutani, Effects of Hydrogen on the Electronic State and Electric Conductivity of the Rutile TiO_2(110) Surface, J. Phys. Soc. Jpn. **84**, 64716 (2015).

[27] Z. Wu, W. Zhang, F. Xiong, Q. Yuan, Y. Jin, J. Yang, and W. Huang, Active hydrogen species on TiO_2 for photocatalytic H_2 production, Phys. Chem. Chem. Phys. **16**, 7051 (2014).

[28] C. Di Valentin, G. Pacchioni, and A. Selloni, Electronic Structure of Defect States in Hydroxylated and Reduced Rutile TiO_2(110) Surfaces, Phys. Rev. Lett. **97**, 166803 (2006).

[29] B. J. Morganand G. W. Watson, A DFT+U description of oxygen vacancies at the TiO_2 rutile (110) surface, Surf. Sci. **601**, 5034 (2007).

[30] G. Mattioli, F. Filippone, P. Alippi, and A. Amore Bonapasta, *Ab initio* study of the electronic states induced by oxygen vacancies in rutile and anatase TiO_2, Phys. Rev. B **78**, 241201(R) (2008).

[31] N. A. Deskins, R. Rousseau, and M. Dupuis, Localized electronic states from surface hydroxyls and polarons in TiO_2(110), J. Phys. Chem. C **113**, 14583 (2009).

[32] J. Stausholm-Moller, H. H. Kristoffersen, B. Hinnemann, G. K. H. Madsen, and B. Hammer, DFT+U study of defects in bulk rutile TiO_2, J. Chem. Phys. **133**, 144708 (2010).

[33] B. J. Morganand G. W. Watson, A Density Functional Theory + U Study of Oxygen Vacancy Formation at the (110), (100), (101), and (001) Surfaces of Rutile TiO_2, J. Phys. Chem. C **113**, 7322 (2009).

[34] B. J. Morganand G. W. Watson, Intrinsic n-type Defect Formation in TiO_2: A Comparison of Rutile and Anatase from GGA+U Calculations, J. Phys. Chem. C **114**, 2321 (2010).

[35] N. A. Deskins, R. Rousseau, and M. Dupuis, Defining the Role of Excess Electrons in the Surface Chemistry of TiO_2, J. Phys. Chem. C **114**, 5891 (2010).

[36] P. Deák, B. Aradi, and T. Frauenheim, Polaronic effects in TiO_2 calculated by the HSE06 hybrid functional: Dopant passivation by carrier self-trapping, Phys. Rev. B **83**, 155207 (2011).

[37] T. Shibuya, K. Yasuoka, S. Mirbt, and B. Sanyal, A systematic study of polarons due to oxygen vacancy formation at the rutile TiO_2(110) surface by GGA+U and HSE06 methods, J. Phys.: Condens. Matter **24**, 435504 (2012).

[38] D. O. Scanlon, C. W. Dunnill, J. Buckeridge, S. A. Shevlin, A. J. Logsdail, S. M. Woodley, C. R. A. Catlow, M. J. Powell, R. G. Palgrave, I. P. Parkin, G. W. Watson, T. W. Keal, P. Sherwood, A. Walsh, and A. A. Sokol, Band alignment of rutile and anatase TiO_2, Nat. Mater. **12**, 798 (2013).

[39] H. Zhu, P. Zhou, X. Li, and J.-M. Liu, Electronic structures and optical properties of rutile TiO_2 with different point defects from DFT+U calculations, Phys. Lett. A **378**, 2719 (2014).

[40] S. Moser, L. Moreschini, J. Jaćimović, O. S. Barišić, H. Berger, A. Magrez, Y. J. Chang, K. S. Kim, A. Bostwick, E. Rotenberg, L. Forró, and M. Grioni, Tunable Polaronic Conduction in Anatase TiO_2, Phys. Rev. Lett. **110**, 196403 (2013).

[41] T. C. Rödel, F. Fortuna, F. Bertran, M. Gabay, M. J. Rozenberg, A. F. Santander-Syro, and P. Le Fèvre, Engineering two-dimensional electron gases at the (001) and (101) surfaces of TiO_2 anatase using light, Phys. Rev. B **92**, 041106 (2015).

[42] M. Setvin, X. Hao, B. Daniel, J. Pavelec, Z. Novotny, G. S. Parkinson, M. Schmid, G. Kresse, C. Franchini, and U. Diebold, Charge Trapping at the Step Edges of TiO_2 Anatase (101), Angew. Chem., Int. Ed. **53**, 4714 (2014).

[43] N. Nagatsuka, M. Wilde, and K. Fukutani, Hydrogenation and hydrogen diffusion at the anatase TiO_2(101) surface, J. Chem. Phys. **152**, 074708 (2020).

[44] S. Ogawa, K. Kato, N. Nagatsuka, S. Ogura, and K. Fukutani, $\sqrt{2} \times \sqrt{2}R45^\circ$ reconstruction and electron doping at the SrO-terminated $SrTiO_3$(001) surface, Phys. Rev. B **96**, 085303 (2017).

[45] Y. Aiura, I. Hase, H. Bando, T. Yasue, T. Saitoh, and D. S. Dessau, Photoemission study of the metallic state of lightly electron-doped $SrTiO_3$, Surf. Sci. **515**, 61 (2002).

[46] K. Takeyasu, K. Fukada, S. Ogura, M. Matsumoto, and K. Fukutani, Two charged states of hydrogen on the $SrTiO_3$(001) surface, J. Chem. Phys. **140**, 084703 (2014).

[47] M. M. Islam, M. Calatayud, and G. Pacchioni, Hydrogen Adsorption and Diffusion on the Anatase TiO_2(101) Surface: A First-Principles Investigation, J. Phys. Chem. C **115**, 6809 (2011).

[48] U. Aschauerand A. Selloni, Hydrogen interaction with the anatase TiO_2(101) surface, Phys. Chem. Chem. Phys. **14**, 16595 (2012).

[49] E. Finazzi, C. Di Valentin, G. Pacchioni, and A. Selloni, Excess electron states in reduced bulk anatase TiO_2: Comparison of standard GGA, GGA+U, and hybrid DFT calculations, J. Chem. Phys. **129**, 154113 (2008).

[50] A. Amore Bonapasta, F. Filippone, G. Mattioli, and P. Alippi, Oxygen vacancies and OH species in rutile and anatase TiO_2 polymorphs, Catalysis Today **144**, 177 (2009).

[51] H. Chengand A. Selloni, Energetics and diffusion of intrinsic surface and subsurface defects on anatase TiO_2(101), J. Chem. Phys. **131**, 054703 (2009).

[52] B. J. Morganand G. W. Watson, Polaronic trapping of electrons and holes by native defects in anatase TiO_2, Phys. Rev. B **80**, 233102 (2009).

[53] K. Yang, Y. Dai, B. Huang, and Y. P. Feng, Density-functional characterization of antiferromagnetism in oxygen-deficient anatase and rutile TiO_2, Phys. Rev. B **81**, 033202 (2010).

[54] T. Yamamotoand T. Ohno, A hybrid density functional study on the electron and hole trap states in anatase titanium dioxide, Phys. Chem. Chem. Phys. **14**, 589 (2012).

[55] M.-A. Haaand A. N. Alexandrova, Oxygen vacancies of anatase (101): Extreme sensitivity to the density functional theory method, J. Chem. Theory Comput. **12**, 2889 (2016).

[56] N. A. Deskins, G. A. Kimmel, and N. G. Petrik, Observation of Molecular Hydrogen Produced from Bridging Hydroxyls on Anatase TiO_2(101), J. Phys. Chem. Lett. **11**, 9289 (2020).

[57] K. Fukutani, Below-surface behavior of hydrogen studied by nuclear reaction analysis, Curr. Opin. Solid State Mater. Sci. **6**, 153 (2002).

[58] M. Wildeand K. Fukutani, Hydrogen detection near surfaces and shallow interfaces with resonant nuclear reaction analysis, Surf. Sci. Rep. **69**, 196 (2014).

[59] J. F. Zieglerand J. P. Biersack, The stopping and range of ions in matter, in *Treatise on Heavy-Ion Science: Astrophysics, Chemistry, and Condensed Matter*, edited by D. A. Bromley (Springer, New York, 1985), Volume 6, pp. 93–129.

[60] PHASE, National Institute for Materials Science [https://azuma.nims.go.jp/software/phase/].

[61] J. P. Perdew, K. Burke, and M. Ernzerhof, Generalized Gradient Approximation Made Simple, Phys. Rev. Lett. **77**, 3865 (1996).

[62] P. Scheiber, M. Fidler, O. Dulub, M. Schmid, U. Diebold, W. Hou, U. Aschauer, and A. Selloni, (Sub)Surface Mobility of Oxygen Vacancies at the TiO_2 Anatase (101) Surface, Phys. Rev. Lett. **109**, 136103 (2012).

[63] M. Cococcioniand S. de Gironcoli, Linear response approach to the calculation of the effective interaction parameters in the LDA + U method, Phys. Rev. B **71**, 035105 (2005).

[64] K. Kato, N. Nagatsuka, and K. Fukutani (unpublished).